

# Interaction Studies of Coumaroyltyramine with Human Serum Albumin and Its Biological Importance

Satyabala Neelam,<sup>†</sup> Mahesh Gokara,<sup>†</sup> Babu Sudhamalla,<sup>†</sup> Damu G. Amooru,<sup>‡</sup> and Rajagopal Subramanyam<sup>\*,†</sup>

Department of Biochemistry, School of Life Sciences, University of Hyderabad, Hyderabad, Andhra Pradesh 500046, India, and Department of Chemistry, Yogi Vemana University, Kadapa, Andhra Pradesh 516003, India

Received: October 24, 2009; Revised Manuscript Received: January 21, 2010

*N-trans-p-Coumaroyltyramine (CT)* isolated from *Physalis minima* is a phenolic substance exhibiting many pharmacological activities like potent inhibition of acetyl cholinesterase, cell proliferation, platelet aggregation, and also antioxidant activity. Here, we have studied the binding of CT with HSA at physiological pH 7.2 by using fluorescence, circular dichroism spectroscopy, mass spectrometry, and molecular docking methods. From the fluorescence emission studies, the number of binding sites and binding constant were calculated to be 2 and  $(4.5 \pm 0.01) \times 10^5 \text{ M}^{-1}$ , respectively. The free energy change was calculated as  $-7.6 \text{ kcal M}^{-1}$  at 25 °C, which indicates the hydrophobic interactions of CT with HSA and is in well agreement with the computational calculations and molecular docking studies. The changes in the secondary structure of HSA after its complexation with the ligand were studied with CD spectroscopy, which indicated that the protein became partially unfolded. Also, temperature did not affect the HSA–CT complexes. The binding of CT with HSA was detected as 2 molecules bound to HSA was determined using micro TOF-Q mass spectrometry. Further, molecular docking studies revealed that CT was binding at subdomain IIA with hydrophobic interactions and also by hydrogen-bond interactions between the hydroxyl (OH) group of carbon-16 and carbon-2 of CT and Arg222, Ala291, Val293, and Met298 of HSA, with hydrogen-bond distances of 2.488, 2.811, 2.678, and 2.586 Å, respectively.

## I. Introduction

Human serum albumin (HSA) is the principal extracellular protein of blood plasma, synthesized and secreted from liver cells.<sup>1,2</sup> It plays an important role in maintaining normal osmolarity in plasma as well as in interstitial fluids. It is a globular protein consisting of a single peptide chain of 585 amino acids, largely helical (~67%) and having 67 kDa mass. It is composed of three structurally homologous domains (I, II, and III), each containing subdomains A and B stabilized by 17 disulfide bridges. Each domain contains 10 helices; helices 1–6 form the respective subdomains A, and helices 7–10 comprise subdomains B. Aromatic and heterocyclic ligands were found to bind within two hydrophobic pockets in subdomains IIA and IIIA, described as site I and site II.<sup>1–7</sup> Seven binding sites are localized for fatty acids in subdomains IB, IIIA, IIIB, and on the subdomain interfaces.<sup>7</sup> HSA has the high affinity metal binding site at the N-terminus.<sup>1</sup> It binds a variety of substrates, including hormones, metal ions, fatty acids, amino acids, and diverse drugs.<sup>1,8,9</sup> The abundance of HSA in the circulatory system and its extraordinary acceptor capabilities makes it an important tool in the prognosis of pharmacokinetic behavior of several drugs.<sup>8,9</sup> It has been shown that the distribution, free concentration, and the metabolism of various drugs can be significantly altered as a result of their binding to HSA.<sup>1</sup> HSA is a widely studied protein because its primary structure is well-known and its tertiary structure has been determined by X-ray

crystallography.<sup>1</sup> There are many reports containing studies on HSA structure and its interactions with different ligands.<sup>10–18</sup> Often, more than 90% of the drugs are bound to the protein, which significantly influences the drug efficacy, the rate of drug delivery, and its elimination. Thus, interactions with plasma proteins, especially HSA, are important factors to be considered in drug development. Very recent reports from our group<sup>19,20</sup> showed that the natural products of pentacyclic triterpenoids, betulinic acid and feruloyl maslinic acid isolated from *Tephrosia calophylla* and *Tetracera asiatica*, respectively, were binding strongly to HSA, leading to ligand–HSA complexation.<sup>19,20</sup>

The importance of phytochemicals is rapidly being recognized, and extensive research is consequently focused on finding their beneficial effects and on evaluating their potential impact on human health. Phenolic substances are widely distributed in the plant kingdom, the products of higher plants secondary metabolism in response to external stimuli. Among these, hydroxycinnamate–tyramine conjugates derived from the phenol propanoid pathway are considered to be defense chemicals that protect plants against pathogen and herbivore attack.<sup>21</sup> Phenolic amides have cytotoxic, anti-inflammatory, antineoplastic, cardiovascular, mild analgesic activity, and antifungal properties.<sup>21</sup> *N-trans-p-Coumaroyltyramine (CT)* is a phenolic amide, mainly produced in plants during wounding and defense mechanisms by the formation of reactive oxygen species during suberization, pathogen attack.<sup>22</sup>

The in vitro studies suggest that CT has the growth suppressing activity of tumor cell lines and arrests the cells at the S-phase of the cell cycle by inhibition of protein tyrosine kinases.<sup>23</sup> CT can inhibit *Mycobacterium tuberculosis* growth rate, and also this compound showed significant inhibitory effects on platelet

\* Corresponding author. Tel.: +91-40-23134572. Fax: +91-40-23010120. E-mail: srgsl@uohyd.ernet.in.

<sup>†</sup> University of Hyderabad.

<sup>‡</sup> Yogi Vemana University.

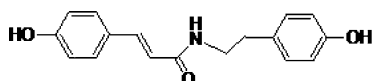


**Figure 1.** Chemical structure of *N*-trans-*p*-coumaroyltyramine. The molecular mass is 283.32 Da, and its molecular formula is C<sub>17</sub>H<sub>17</sub>NO<sub>3</sub>.

aggregation.<sup>24</sup> CT had also shown potent radical scavenging activity. In vivo studies indicated that CT has the inhibitory effects on acetyl cholinesterase, an enzyme responsible for the metabolic hydrolysis of acetylcholine. The use of ach inhibitors is an important therapeutic strategy for activating central cholinergic functions in Alzheimer's disease.<sup>25</sup> Also, it is a potent  $\alpha$ -glucosidase inhibitor,<sup>26</sup> and CT can inhibit P-selectin expression on platelets through COX inhibition.<sup>27</sup>

*Physalis minima* (Solanaceae) is widely distributed throughout tropical and subtropical regions of the world. *Physalis* species have been widely used in folk medicine as anticancer, antimycobacterial, antileukemic, antipyretic, and immunomodulatory substances, and also were used to cure the diseases such as malaria, asthma, hepatitis, dermatitis, diuretic, and rheumatism.<sup>28,29</sup> In the present study, analysis and comparison of the <sup>1</sup>H NMR and <sup>13</sup>C NMR spectra of a compound from the methanol extract of *P. minima*, with published data,<sup>30</sup> allowed the identification of the compound as *N*-trans-*p*-coumaroyltyramine. The molecular mass is 283.32 Da, and its molecular formula is C<sub>17</sub>H<sub>17</sub>NO<sub>3</sub> (Figure 1).

Although *N*-trans *p*-coumaroyltyramine has been identified and characterized in plants, its biological effects on human cells have not been investigated due to its low concentration in plants. Because of the fact that CT has several beneficial medicinal properties, a study of its interactions with the major carrier protein like HSA is essential. Thus, we present here the study of interactions and protein conformation of HSA with *N*-trans-*p*-coumaroyltyramine under physiological conditions using fluorescence, microTOF-Q mass spectrometry, circular dichroism (CD), and molecular docking studies.

## II. Material and Methods

**A. Isolation and Identification of *N*-trans-*p*-Coumaroyltyramine.** The dried whole plants of *P. minima* (9.4 kg) (collected from south India) were extracted with MeOH (8 × 16 L) under reflux. The combined extracts were concentrated under reduced pressure to give a dark brown extract (580 g). This extract was suspended in H<sub>2</sub>O and partitioned with CHCl<sub>3</sub> and *n*-BuOH, successively. The CHCl<sub>3</sub> soluble extracts (96 g) were separated over a column containing silica gel and eluted with *n*-hexane/ethyl acetate mixtures with increasing proportions of ethyl acetate to afford 10 fractions. A series of chromatographic separations of fraction 5 with *n*-hexane/ethyl acetate mixtures and a gradient of chloroform and isopropyl ether as eluants yielded (182 mg) pure *N*-trans-*p*-coumaroyltyramine. The purity of the CT was confirmed by MALDI-TOF mass spectrometry, and the single peak appeared to correspond with the mass of 283 Da (data not shown).

**B. Preparation of Stock Solutions.** Pure fat-free human serum albumin (a kind gift from Virchow Biotech Pvt Ltd., Hyderabad) was dissolved in an aqueous solution of 0.1 M physiological phosphate buffer, pH 7.2. The stock solution of CT was prepared in 0.6% DMSO and had a concentration of 1.5 mM. The effect of 0.6% DMSO has a negligible effect on the structure of HSA (data not shown). The time of CT binding to HSA was examined via fluorescence emission and CD spectra, and it was found that 10 min was the maximum binding time, and hence the incubation of CT was fixed at 10 min in all studies.

**C. Fluorescence Spectroscopy.** The fluorescence emission spectra were recorded on a Jobin-Yvon, FluoroMax-3 instrument, with excitation at 285 nm; the slit width for excitation and emission was 5 nm. Emission spectra were recorded between 300 and 500 nm. The sample temperature was maintained at 25 °C. HSA concentration was 0.025 mM, and the concentrations of CT were 0.006, 0.016, 0.033, 0.050, 0.066, 0.076, 0.099, 0.110, and 0.133 mM in 0.1 M phosphate buffer, pH 7.2 (physiological pH). During the course of our experiments, the CT compound appeared as a minor shoulder around 450 nm wavelength. Three independent experiments were performed, and identical spectra were obtained.

**D. Circular Dichroism Spectroscopy.** CD spectra of free HSA and HSA-CT samples were recorded with JASCO-810 spectropolarimeter. For measurements in the far-UV region (180–260 nm), a quartz cell with a path length of 0.2 mm was used. Three scans were accumulated with continuous scan mode and a scan speed of 50 nm min<sup>-1</sup> with data being collected at every nanometer. The sample temperature was maintained at 25 °C. The protein concentration was fixed to 0.025 mM, and the CT concentrations used were 0.01, 0.05, and 0.1 mM in 0.1 M phosphate buffer, pH 7.2. Sample temperatures were maintained using circulating water bath connected to water jacketed quartz cuvettes. Protein secondary structure was calculated using CDNN 2.1 software. An ellipticity of CD spectra is expressed in millidegrees.

**E. Electrospray Ionization Mass Spectrometry (Micro TOF-Q).** Positive ion mode mass spectra were recorded on a micro TOF-Q (Bruker Daltonics, Bremen, Germany) equipped with an electrospray ionization source. For these measurements, the HSA concentration used was 0.15 μM, and the CT concentrations were 0.1, 0.2, 0.3, 0.4, and 0.5 μM. Free HSA and HAS-CT were prepared in 5 mM ammonium acetate (pH 7.2) mixed with 20% acetonitrile and introduced into the mass spectrometer source with a syringe pump (KD Scientific Inc., Billerica, MA) at 3 μL/min. Electrospray was performed by setting the spray voltage at 4.5 kV. The time-of-flight (TOF) pressure was maintained at less than 3 × 10<sup>-7</sup> Torr. Scanning was performed over an *m/z* range of 50–3000, with a collision energy of 10 eV. Data were averaged for 2 min and then smoothed using the Gaussian algorithm in the Bruker Data Analysis 3.4 software program. The instrument was calibrated using ES tuning mix (Agilent Technologies, part no. G2421-60001) and injected through a divert valve just before sample application.

**F. Molecular Modeling and Docking. Genetic Algorithm.** GOLD (genetic optimization for ligand docking), a docking program based on genetic algorithm,<sup>31</sup> was used to dock the ligands to the protein active sites. Genetic algorithm is a computer program that mimics the process of evolution by structures called chromosomes. Each of these encodes a possible solution (in terms of a possible ligand–receptor interaction) to the docking problem and may be assigned a fitness score on the basis of the relative merit of that solution. Each chromosome encodes an internal conformation and protein active site and includes a mapping from hydrogen bonding sites in the ligand and protein. On decoding a chromosome, a least-squares fitting process is employed to position the ligand within the active site of the protein. The fitness of a decoded chromosome is then a combination of the number and strength of the hydrogen bonds that have been formed in this way and of the van der Waals energy of the bound complex.

**Preparation of the Protein and the Ligand.** The known crystal structure of HSA (PDB ID: 1AO6) was obtained from the Brookhaven Protein Data Bank. From the 2D structure, the

three-dimensional structure of CT was built, and the geometry was optimized through the discover3 in InsightII/Builder program. Water molecules and ions were removed (including ordered water molecules), and hydrogen atoms added at appropriate geometry and groups within the protein were ionized as required at physiological pH. The structure of HSA was protonated in InsightII ([www.accelrys.com](http://www.accelrys.com)). Genetic algorithm was implemented in GOLDv3.2 that was applied to calculate the possible conformations of the drug that binds to the protein. During the docking process, a maximum of 10 different conformations were considered for the drug. Among them, we have used the lowest binding free energy for further analysis according to Qiu and Yi.<sup>32</sup>

**AutoDock.** AutoDock generated the different ligand conformers using a Lamarkian genetic algorithm (LGA), a GA implementation with an adaptive local method search.<sup>33</sup> The simulations started with a predefined number of generation cycles, composed of mapping and fitness evaluation, selection, crossover, mutation, and elitist selection steps, and continued with a local search, followed by the scoring of the generated conformers. The energy-based AutoDock scoring function includes terms accounting for short-range van der Waals and electrostatic interactions, loss of entropy upon ligand binding, hydrogen bonding, and solvation. The protein and the ligand input structures, prepared as described above, were transformed into corresponding pdbq format files (containing atom coordinates, partial charges, and solvation parameters), with the mol2- to pdbqs and AutoTors programs, respectively. The ligand-centered maps were generated by the program auto grid with a spacing of 0.375 Å and dimensions of 60 × 60 × 60 points. The ligand rigid roots were automatically set, and all possible rotatable bonds and torsions were defined as active. All other parameters were as set by default. For each docking simulation, 10 different conformers were generated.

### III. Results and Discussion

**A. Fluorescence Quenching of HSA by CT.** Fluorescence quenching of the protein could be used to retrieve information about many drug–protein binding interactions.<sup>34</sup> The emission fluorescence of HSA comes from tryptophan, tyrosine, and phenylalanine. Phenylalanine has a very low quantum yield, and the fluorescence of tyrosine is almost totally quenched if it is ionized or present near an amino group, a carboxyl group, or a tryptophan. Hence, the fluorescence of HSA is practically composed of the tryptophan emission alone, and the emission spectrum of HSA is mainly from a single tryptophan residue located at the 214 position in subdomain IIA. The changes of the intrinsic fluorescence intensity of HSA were due to the tryptophan residue when small molecules bound to HSA.<sup>35</sup> Addition of increasing concentrations of CT (0.006–0.133 mM) to fixed protein (HSA) concentration (0.025 mM) resulted in fluorescence quenching, which can be observed in Figure 2A. This indicates that CT–HSA complexes were formed upon interaction of CT with HSA and lead to microenvironment changes in the protein. Similar fluorescence results were reported for several ligands.<sup>10–18,36,37</sup> Also, fluorescence titration spectra at room temperature show the shift of  $\lambda_{\text{max}}$  to higher wavelengths with increasing concentration of the ligand. These results indicate that there is a shift of the sole tryptophan residue to a more polar environment on ligand binding to HSA.<sup>14,36,37</sup>

The decrease of fluorescence intensity is known as quenching, which may be due to the interaction of the excited state of the fluorophore with its surroundings.<sup>38</sup> The fluorophore here is the Trp 214, and the change of fluorescence intensity is due

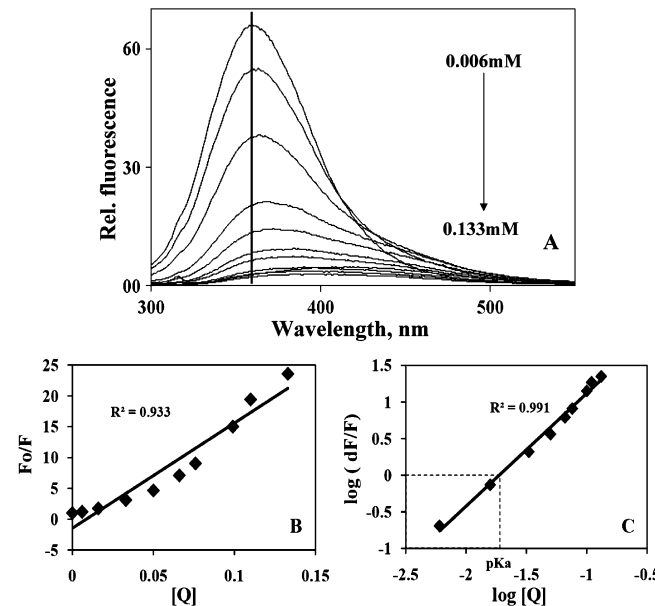


**Figure 2.** Room-temperature fluorescence emission spectra of HSA–CT in 0.1 M phosphate buffer pH 7.2. (A) Free HSA (0.025 mM) and free HSA with different concentrations of CT (0.006, 0.016, 0.033, 0.050, 0.066, 0.076, 0.099, 0.110, 0.133 mM). (B) Plot of  $F_0/F$  against  $[Q]$ .  $\lambda_{\text{ex}} = 285 \text{ nm}$ ,  $\lambda_{\text{em}} = 362 \text{ nm}$ . (C) Logarithmic plot of fluorescence quenching of HSA treated with different CT concentrations (0.006–0.133 mM). The  $pK_a$  value was obtained from the X axis where perpendicular dropped from the intercept meets, and the binding constant corresponds to  $1/K_{\text{CT}} = K_{\text{CT}} = 1/10^{pK_a}$ . For further details, see the experimental section.

to the interactions of the HSA with CT. The CT may be interacting with its phenolic hydroxyl groups of the HSA. Tryptophan residues are highly sensitive to the local environments, and changes in the emission spectra of tryptophan are common in response to protein conformational changes and substrate binding. This viewpoint was well supported by the experimental observations of Sulkowska<sup>35</sup> and Lakowicz.<sup>38</sup> The compound CT has a fluorescence peak in the range of 440–500 nm; however, in the lower concentrations of CT, the CT fluorescence maximum is not seen clearly.

**B. Calculation of Binding Constant.** The binding constant can be calculated from the Stern–Volmer law of fluorescence quenching:

$$F_0/F = 1 + K^*[Q] \quad (1)$$

where  $F_0$  and  $F$  are the fluorescence intensities of HSA in the absence of CT and various concentrations of CT. A plot of  $F_0/F$  versus  $[Q]$  should give a linear relationship<sup>39</sup> if it is a one-to-one interaction between the protein and ligand. The result here (Figure 2b) is a nonlinear relationship indicating that the interaction between HSA and CT is not a one-to-one interaction. To see multiple binding sites on the protein, the Stern–Volmer plot can be transformed into the following equation:<sup>10,40</sup>

$$\log[(F_0 - F)/F] = \log K_S + n * \log(Q) \quad (2)$$

where  $n$  is the slope that corresponds to the number of binding sites,  $K_S$  is the binding constant, and  $Q$  is the quencher concentration. The results indicated a good linear relationship with a slope of 1.538, indicating that about two molecules of CT were bound to HSA. The binding constant  $K_{\text{CT}}$  was

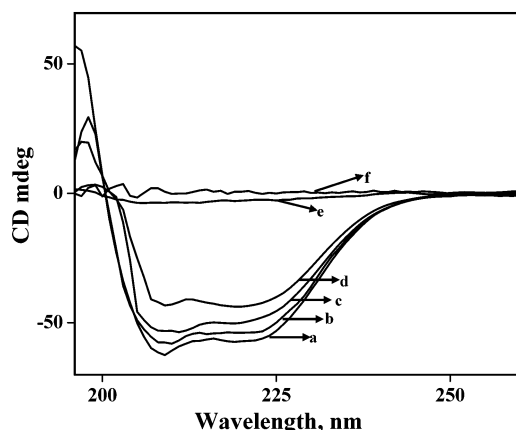


**Figure 3.** Circular dichroism spectra of the free HSA and its CT analogue complexes in aqueous solution with a protein concentration of 0.025 mM and CT concentrations from 0.01, 0.05, 0.1 mM. (a) Free HSA, (b) HSA+0.01 mM CT, (c) HSA+0.05 mM CT, (d) HSA+0.1 mM CT, (e) phosphate buffer, and (f) 0.1 mM CT only.

**TABLE 1: Secondary Structural Analysis of the Free HSA and Its Interaction with CT<sup>a</sup>**

	free HSA	HSA+0.01 mM CT	HSA+0.05 mM CT	HSA+0.1 mM CT
helix (%)	58.1 ± 2.5	55.8 ± 2.5	42.9 ± 2.9	35.7 ± 3.0
antiparallel (%)	2.9 ± 0.3	3.2 ± 0.4	5.9 ± 0.41	8.6 ± 0.45
parallel (%)	4.1 ± 0.5	4.3 ± 0.55	6.3 ± 0.6	7.6 ± 0.6
β-turn (%)	19.0 ± 0.8	19.4 ± 0.82	20.8 ± 0.81	20.2 ± 1.0
random coil (%)	15.9 ± 0.7	17.3 ± 0.7	24.1 ± 0.8	27.9 ± 0.99

<sup>a</sup> Based on Figure 3, with the data analyzed by web-based software CDNN 2.1.

calculated from the intercept as  $(4.5 \pm 0.01) \times 10^5 \text{ M}^{-1}$  (intercept =  $\log K$ ), which indicates strong binding of CT to HSA. In our recent reports, the isolated betulinic acid and feruloyl maslinic acid isolated from *Tephrosia calophyllum* and *Tetracera asiatica* were showing binding constants of  $K_{BA} = (1.685 \pm 0.01) \times 10^6 \text{ M}^{-1}$  and  $K_{FMA} = (1.42 \pm 0.01) \times 10^8 \text{ M}^{-1}$ .<sup>19,20</sup> Thus, our results show clearly that CT is strongly binding to the HSA and forms the ligand–protein complexes. Most of the natural compounds like flavonoids display binding constants in the range of  $(1\text{--}15) \times 10^4 \text{ M}^{-1}$ .<sup>41</sup> Quercitin (flavonoid) binds with an affinity of  $1.46 \times 10^4 \text{ M}^{-1}$ ,<sup>40</sup> while resveratrol, a polyphenol, binds with an affinity of  $1.64 \times 10^5 \text{ M}^{-1}$ .<sup>42</sup>

**C. Free Energy Calculations.** The standard free energy changes are calculated according to the equation:

$$\Delta G^0 = -RT \ln K \quad (3)$$

where  $\Delta G$  is free energy,  $K$  is binding constant at the corresponding temperature, which can be obtained from fluorescence data, and  $R$  is the universal gas constant. Thus, the standard free energy change calculated accordingly ( $\Delta G^0 = -RT$

$\ln K$ ) obtained was  $-7.6 \text{ kcal/mol}$  at  $25^\circ\text{C}$  for the binding of CT to HSA. The negative value of the free energy of binding CT to HSA is mainly by hydrophobic and possibly hydrogen-bond interactions.

**D. CD Spectroscopic Studies.** To observe the CT–HSA complexation and its effects on the secondary structure of protein, CD measurements were performed on free HSA and HSA–CT systems at room temperature. HSA exhibits two negative peaks, which is the characteristic feature of α-helix structure in the UV region at 208 and 222 nm. Free HSA has 58% α-helix content, 26% β-sheets content, and 16% random coil content, which is in agreement with the previous reports.<sup>19,20,40–45</sup> Indeed, the original crystal structure showed the 67% of α-helical;<sup>2</sup> however, in our case it was 58% of α-helical content. The differences in α-helical contents can be attributable to the different structural arrangements of the protein in the solid state (X-ray structure) and in aqueous solution (CD measurements). Structural differences were also observed for other proteins in the solid state and in aqueous solution.<sup>46–48</sup> A noticeable change in the secondary structure of HSA was observed with increasing concentrations of CT (Figure 3). At 0.01 mM concentration, there was a little change in the secondary structure of the protein. However, at 0.1 mM concentration, α-helix content was decreased to 35.7%, and β-sheets and random coil contents were increased to 36.5% and 27.9%, respectively, indicating that there is a partial destabilization of the α-helix, which clearly reveals the conformational changes in the protein secondary structure upon complexation with CT. These results indicated that the secondary structure of HSA became partially unfolded due to HSA–CT complex formation. The secondary structural conformational changes appear likely because some inherent flexibility due to binding of CT molecule to HSA at IIA domain and also an additional binding of second molecule of CT to HSA could cause conformational changes. Consequently, we see in our data that the CD changes upon binding of CT to HSA. Similar results were observed on binding of other ligands (pentacyclic triterpenoids, betulinic acid, feruloyl maslinic acid, flavonoids, quercetin, crocetin, dimethylcrocetin, safranal, retinol, retinoic acid, and resveratrol aliphatic acid) to HSA, causing a major decrease of α-helix and increase of β-sheets and random coils as well.<sup>19,20,40–45</sup> For a reference, polyamine analogues binding to HSA showed the change in protein secondary structure, a major alteration with a reduction of α-helix from 55% (free protein) to 43% and an increase of β-sheet from 17% (free protein) to 29–36% in the 333, BE-333, and BE-3333 complexes, indicating partial protein unfolding upon polyamine interaction.<sup>44</sup>

To check the thermal stability of the HSA and HSA–CT complexes (which contained 0.1 mM of CT with 0.025 mM HSA), the temperature-dependent CD spectra were measured from 30 to  $70^\circ\text{C}$ . With increasing temperature, there was no change in protein unfolding of HSA and HSA–CT complexes up to  $60^\circ\text{C}$ , and further there were marginal changes in the secondary structural conformations (Tables 2 and 3). It is interesting to observe that free HSA undergo conformational

**TABLE 2: Secondary Structural Analysis of Free HSA Alone at Different Temperatures**

	HSA 30 °C	HSA 40 °C	HSA 50 °C	HSA 60 °C	HSA 70 °C
helix (%)	58.1 ± 2.4	58.1 ± 2.4	57.6 ± 2.4	55.4 ± 2.4	45.0 ± 2.4
antiparallel (%)	2.9 ± 0.3	2.8 ± 0.3	3.2 ± 0.3	4.0 ± 0.3	6.6 ± 0.35
parallel (%)	4.1 ± 0.5	4.0 ± 0.5	4.4 ± 0.5	4.9 ± 0.5	6.3 ± 0.6
β-turn (%)	18.9 ± 0.7	19.1 ± 0.7	17.4 ± 0.8	16.5 ± 0.6	19 ± 0.8
random coil (%)	16.0 ± 0.7	16.0 ± 0.7	17.4 ± 0.7	19.2 ± 0.7	23.1 ± 0.8

**TABLE 3:** Secondary Structural Analysis of HSA–CT Complexes (HSA+0.1 mM CT) at Different Temperatures from 30 to 70 °C

	HSA+CT 30 °C	HSA+CT 40 °C	HSA+CT 50 °C	HSA+CT 60 °C	HSA+CT 70 °C
helix (%)	35.7 ± 3.0	35.2 ± 2.99	34.6 ± 2.27	33.3 ± 2.38	28.0 ± 1.0
antiparallel (%)	8.6 ± 0.5	8.6 ± 0.5	9.2 ± 0.6	9.0 ± 0.5	13.8 ± 0.8
parallel (%)	7.6 ± 0.6	7.8 ± 0.6	8.0 ± 0.6	8.2 ± 0.65	9.0 ± 0.69
β-turn (%)	20.2 ± 1.3	19.4 ± 1.0	19.1 ± 1.0	19.3 ± 1.0	18.0 ± 0.9
random coil (%)	27.9 ± 1.5	29.0 ± 2.0	29.1 ± 2.0	29.2 ± 2.0	30.9 ± 2.2

change from 60 °C. The previous report shows that the  $T_m$  of the HSA alone was around 60 °C, which shows that the unfolding of protein occurs only from this point.<sup>49</sup> These results indicate that the HSA–CT complexes were not affected by temperature and thus HSA–CT complexes were conformationally more stable, which indicated that CT bound more tightly to HSA.

**E. Micro TOF-Q Analysis.** Mass spectrometry is often used in pharmacokinetics study due to its high sensitivity in detecting

the compounds at low concentrations. Protein–ligand complexation at micromolar levels was demonstrated using micro TOF-Q mass spectrometry. The mass spectra of free HSA and HSA–CT complexes can be observed in Figure 4A and B. The numbers on dark blue vertical lines indicate the matched charge states of HSA, HSA–CT complexes. Deconvolution of the multiple charged states resulted in the mass determinations of HSA and HSA–CT complexes. In our experiments, we have used a fixed concentration of 0.15 μM of HSA and different concentrations

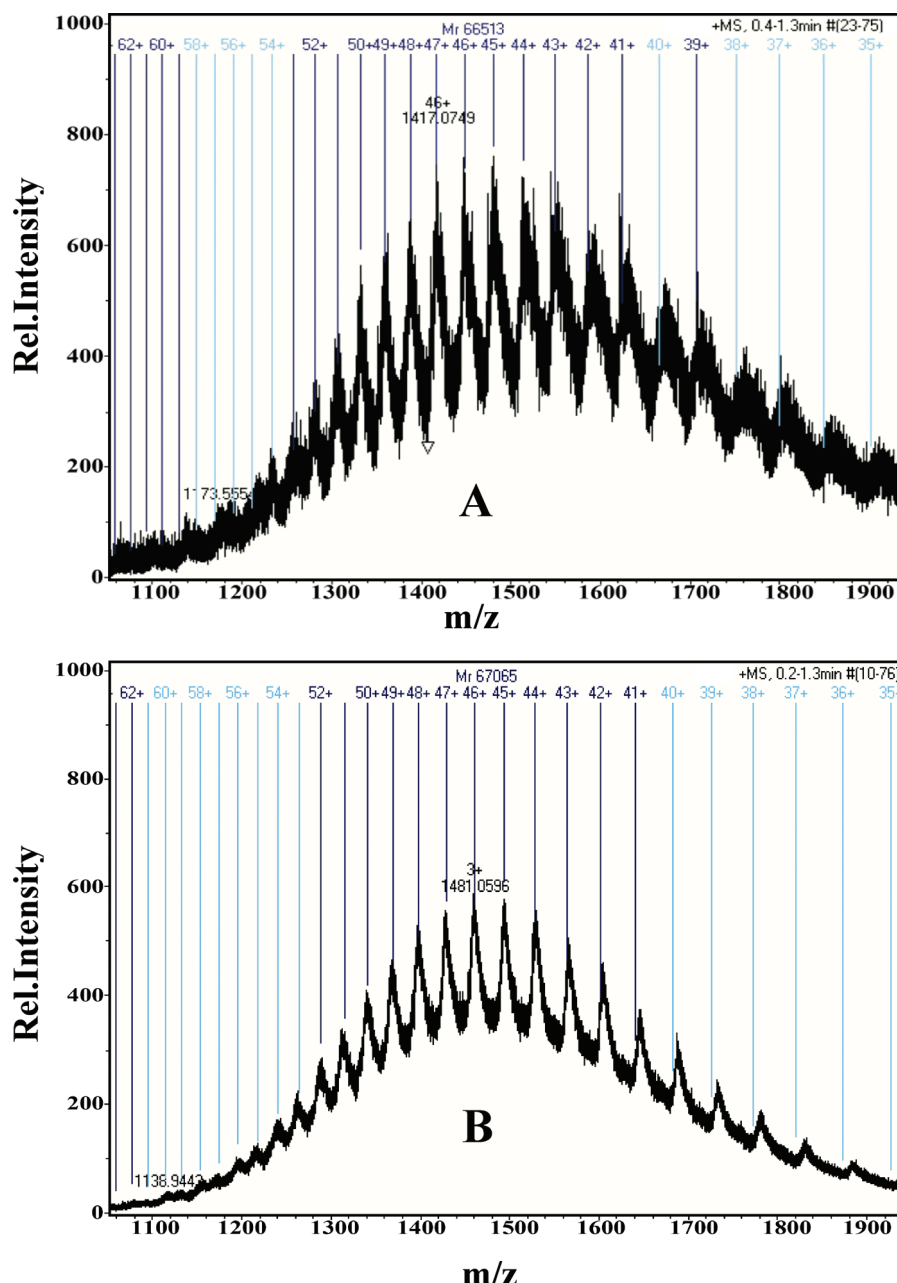


**Figure 4.** (A) Micro TOF-Q mass spectra of free HSA and (B) HSA along with CT. The concentrations of free HSA and CT were 0.15 and 0.5 μM, respectively.  $m/z$ ,  $m$  is mass and  $z$  is charge of the molecule. For further details, see section II.E.

**TABLE 4: Docking Summary of HSA with *N*-trans-p-Coumaroyltyramine by AutoDock Program Generated Different Ligand Conformers Using a Lamarkian Genetic Algorithm<sup>a</sup>**

rank	run	binding energy [kcal M <sup>-1</sup> ]	$K_i$	$K_a$ [M <sup>-1</sup> ]	cluster rmsd	reference rmsd
1	8	<b>-6.02</b>	<b>38.54 μM</b>	<b>2.6 × 10<sup>4</sup></b>	<b>0.00</b>	<b>54.36</b>
2	5	-5.88	49.26 μM	2.03 × 10 <sup>4</sup>	0.00	48.25
3	3	-5.84	52.05 μM	1.92 × 10 <sup>4</sup>	0.00	41.24
4	6	-5.82	54.55 μM	1.83 × 10 <sup>4</sup>	0.00	50.84
5	9	-5.62	75.51 μM	1.32 × 10 <sup>4</sup>	0.00	55.77
6	7	-5.12	175.60 μM	5.70 × 10 <sup>3</sup>	0.00	45.15
7	1	-5.09	184.72 μM	5.41 × 10 <sup>3</sup>	0.00	45.44
8	4	-5.08	190.09 μM	5.26 × 10 <sup>3</sup>	0.00	36.79
9	2	-4.78	311.59 μM	3.20 × 10 <sup>3</sup>	0.00	43.55
10	10	-4.51	497.03 μM	2.01 × 10 <sup>3</sup>	0.00	38.65

<sup>a</sup> The bold font indicates the lowest free energy, which is the more stable model.

of CT (0.1, 0.2, 0.3, 0.4, and 0.5 μM). When analyzing the HSA–CT sample, an increase of molecular mass from 66 513 to 67 065 Da was observed, and this indicated that CT was bound to HSA. The molecular weight of CT being 283.32 Da, the additional mass of 552 Da on HSA was originated because of two molecules of CT. Beyond 0.2 μM of CT concentration, about 2 molecules were bound to HSA, and thus additional binding of CT molecule to HSA was perhaps due to a nonspecific binding. Further, we present here 0.15 μM of HSA and 0.5 μM of CT in Figure 4B for HSA+CT complexes. Also, our fluorescence data support the inference that the interaction of CT to HSA is 2:1. In other reports, the interaction of different ligands like retinoic acid, retinal bound to HSA was 2:1. Also, in another study, the interaction of cucurbitacins with HSA, where the concentration of cucurbitacins and HSA was 1 μM each, the ratio was 2:1 for interaction of cucurbitacins with HSA.<sup>50</sup>

**F. Molecular Docking.** The crystal structure of HSA with numerous ligands has been described.<sup>8</sup> The 3D structure of crystalline HSA revealed the principal regions of ligand binding located in hydrophobic cavities in subdomains IIA and IIIA, which are consistent with site I and site II, respectively.<sup>1–7</sup> In the present data, the GOLD v3.2 AutoDock programs were chosen to examine the binding mode of different ligands at the active site of HSA. During the docking process, 10 conformations were obtained, and among them the lowest free energy solution was chosen for our CT modeling (Table 4). Thus, the best score-ranked result is shown in Figure 5A, which has the lowest free energy. The docking results showed that CT binds within the binding pocket of subdomain IIA. The inside wall of the pocket of subdomain IIA is formed by hydrophobic side chains, whereas the entrance of the pocket is surrounded by positively charged residues consisting of Arg257, Arg222, Lys199, His242, Arg218, and Lys195.<sup>51</sup> It can be seen that the CT molecule was penetrating deep within subdomain IIA hydrophobic cavity (see Figure 5A). The CT molecule moiety was located within the binding pocket, and the coumaroyl chain of CT was adjacent to hydrophobic residues Arg(218), Trp(214), Arg(222), Ala(291), Val(293), etc., of subdomain IIA of HSA (site 1). Thus, we can conclude that the interaction of CT with HSA is mainly hydrophobic, which is in perfect agreement with thermodynamic results (see section III.C). Furthermore, there were also a number of specific electrostatic interactions and hydrogen bonds, because several ionic and polar residues in the proximity of the ligand play an important role in stabilizing the CT molecule via H-bonds and electrostatic interactions. Consequently, there were hydrogen-bonding interactions between the phenolic hydroxyl (OH) group of carbon-16 and carbon-2 of p-CT and Arg(222), Val(293), Ala(291), and Met(298) of HSA, with hydrogen-bond distances of 2.488,

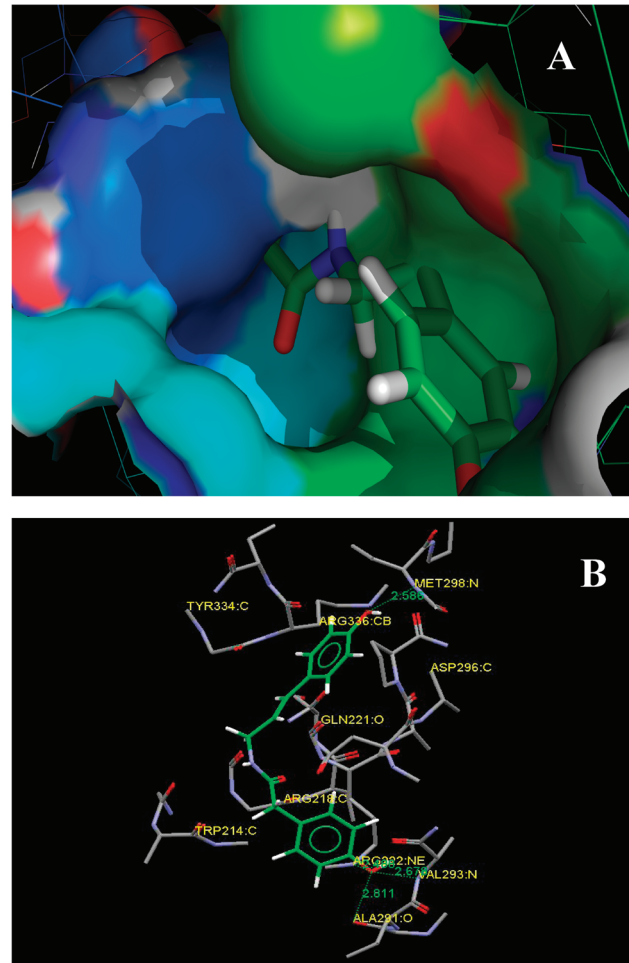


**Figure 5.** (A) CT docked in the binding pocket of HSA using GOLDv3.2. CT depicted in stick model (light green), and HSA represented in solid (better) with ray model. The image was made using Pymol (pymol.sourceforge.net). (B) Stereoview of the docking poses of HSA–CT complex (prepared by using SILVERv1.1.1 visualizer); CT is rendered as capped sticks, and the residues are rendered as ellipsoid model. Four H-bonds (as highlighted by the dashed lines in green color) were formed between CT and HSA.

2.811, 2.678, and 2.586 Å, respectively (see Figure 5B). The results suggested that the formation of hydrogen bonds decreased the hydrophilicity and increased the hydrophobicity to stabilize the CT–HSA complexes. The free energy change  $\Delta G^\circ$  of the binding of CT to HSA is -6.02 kcal/mol, and the binding constant is  $2.60 \times 10^4$  M<sup>-1</sup>. However, the computational results were a little bit different from the experimental results (-7.6 kcal/mol,  $K_{CT} = 4.5 \times 10^5$  M<sup>-1</sup>). Similar results were observed

in different ligands binding to HSA, those of 8-acetyl-7-hydroxycoumarin and naringin binding to HSA.<sup>52,53</sup> The probable explanation for this is the X-ray structure of the protein from crystals is different from that of the aqueous system used in the study, which results in the difference of the microenvironment around the ligand.<sup>52,53</sup> It is easy to draw a conclusion that it would lead to the difference of the binding ability of the protein with the ligand. Obviously, the binding constant  $K$  ( $2.60 \times 10^4 \text{ M}^{-1}$ ) from computational modeling may be not so close to the experimental data ( $K_{CT} = 4.5 \times 10^5 \text{ M}^{-1}$ ) in some way. Therefore, the results of molecular docking indicated that the hydrophobic interactions exist between CT and HSA. It was important to note that the Trp-214 residue of HSA located in drug site 1 (subdomain IIA) was in close proximity to the drug molecule. This finding provided a good structural basis to correlate the results with that of the fluorescence quenching data of HSA emission spectra in the presence of CT.

#### IV. Conclusions

Plant product *N*-trans-*p*-coumaroyltyramine from *Physalis minima* binds to HSA with a binding affinity of  $CT = (4.5 \pm 0.01) \times 10^5 \text{ M}^{-1}$ , and 2 molecules of CT were binding to the protein. The free energy change was calculated to be  $-7.6 \text{ kcal M}^{-1}$  at  $25^\circ\text{C}$ . Further, from CD studies, it was evident that at lower concentrations of CT the protein conformational changes were marginal, whereas at high concentrations of CT, unfolding of the protein with a significant decrease in the  $\alpha$ -helix and an increase in  $\beta$ -turn and random coil were observed upon complexation with the CT. MicroTOF-Q mass spectrometry data suggest 2 molecules of CT were binding to HSA, which also in agreement with the fluorescence data reveals that the interaction of CT with HSA is 2:1. Molecular modeling results suggested that CT mainly binds to HSA at IIA domain on drug site I in hydrophobic pockets with hydrogen-bonding interactions between the phenolic hydroxyl (OH) group of carbon-16 and carbon-2 of p-CT and Arg(222), Val(293), Ala(291), and Met(298) of HSA, with hydrogen-bond distances of 2.488, 2.811, 2.678, and 2.586 Å, respectively. Henceforth, CT has a strong binding interaction with the HSA. Thus, the study of this compound would be useful so as to understand the pharmaceutical agent to cure many diseases.

**Acknowledgment.** We thank Dr. N. Sreepadh, Virchow Biotech, and Hyderabad, India, for a kind gift of pure HSA. We thank Prof. Abani Bhuyan, Department of Biotechnology and Chemistry, University Hyderabad, India, and Prof. P. Mohanty, Jawaharlal Nehru University, New Delhi, India, for invaluable discussions. Also, we thank Mr. Mark Hunter, Arizona State University, for critical reading of the manuscript. We greatly acknowledge the School of Life Sciences, UOH-CREBB, for providing the facility of micro TOF-Q mass spectrometry at the University of Hyderabad. We thank CMSD and CIL for computational and CD facilities at the University of Hyderabad, respectively.

#### References and Notes

- (1) Peters, T. All About Albumin. *Biochemistry, Genetics and Medical Applications*; Academic Press: San Diego, CA, 1996.
- (2) He, H. M.; Carter, D. C. *Nature* **1992**, *358*, 209–215.
- (3) Curry, S.; Mandelkow, H.; Brick, P.; Franks, N. P. *Nat. Struct. Biol.* **1998**, *5*, 827–835.
- (4) Curry, S.; Brick, P.; Frank, N. P. *Biochim. Biophys. Acta* **1999**, *1441*, 131–140.
- (5) Sugio, S.; Kashima, A.; Mochizuki, S.; Noda, M.; Kobayashi, K. *Protein Eng.* **1999**, *12*, 439–446.
- (6) Bhattacharya, A. A.; Curry, S.; Franks, N. P. *J. Biol. Chem.* **2000**, *275*, 38731–38738.
- (7) Petitpas, I.; Grune, T.; Bhattacharya, A. A.; Curry, S. *J. Mol. Biol.* **2001**, *314*, 955–960.
- (8) Ghuman, J.; Zunszain, P. A.; Petitpas, I.; Bhattacharya, A. A.; Otagiri, M.; Curry, S. *J. Mol. Biol.* **2005**, *353*, 38–52.
- (9) Varsnay, A.; Sen, P.; Ahmad, E.; Rehan, M.; Subbarao, N.; Khan, R. H. *Chirality* **2010**, *22*, 77–87.
- (10) Ahmad, B.; Parveen, S.; Khan, R. H. *Biomacromolecules* **2006**, *7*, 1350–1356.
- (11) He, W.; Li, Y.; Si, H.; Dong, Y.; Sheng, F.; Yao, X.; Hu, Z. *J. Photochem. Photobiol.* **2006**, *182*, 158–167.
- (12) Karnaughova, E. *Biochem. Pharmacol.* **2007**, *73*, 901–910.
- (13) Sinha, S. S.; Mitra, R.; Pal, S. K. *J. Phys. Chem.* **2008**, *112*, 4884–4891.
- (14) Maiti, T. K.; Ghosh, K. S.; Samanta, A.; Dasgupta, S. *J. Photochem. Photobiol.* **2008**, *194*, 297–307.
- (15) He, Y.; Wang, Y.; Tang, L.; Liu, H.; Chen, W.; Zheng, Z.; Zou, G. *J. Fluoresc.* **2008**, *18*, 433–442.
- (16) Charbonneau, D.; Beauregard, M.; Tajmir-Riahi, H. A. *J. Phys. Chem.* **2009**, *113*, 1777–1784.
- (17) Li, J.; Liu, X.; Ren, C.; Li, J.; Sheng, F.; Hu, Z. *J. Photochem. Photobiol.* **2009**, *94*, 158–163.
- (18) Yue, Y.; Chen, X.; Qin, J.; Yao, X. *J. Pharm. Biomed. Anal.* **2009**, *49*, 753–759.
- (19) Subramanyam, R.; Gollapudi, A.; Bonigala, P.; Chinnaboina, M.; Amooru, D. G. *J. Photochem. Photobiol., B* **2008**, *94*, 8–12.
- (20) Subramanyam, R.; Goud, M.; Sudhamalla, B.; Reddeem, E.; Gollapudi, A.; Nellaepalli, S.; Yadavalli, V.; Chinnaboina, M.; Amooru, D. G. *J. Photochem. Photobiol., B* **2009**, *95*, 81–88.
- (21) Ishiara, A.; Kawata, N.; Matsukawa, T.; Iwamura, H. *Biosci. Biotechnol. Biochem.* **2000**, *64*, 1025–1031.
- (22) Razem, F. A.; Bernards, M. A. *J. Exp. Bot.* **2003**, *54*, 935–941.
- (23) Park, B. J.; Schoene, N. *Biochem. Biophys. Res. Commun.* **2002**, *292*, 1104–1110.
- (24) Mata, R.; Morales, I.; Perez, O.; Rivero-Cruz, I.; Acevedo, L.; Enriquez-Mendoza, I.; Bye, R.; Franzblau, S.; Timmermann, B. *J. Nat. Prod.* **2004**, *67*, 1961–8.
- (25) Kim, D. K.; Lee, K. *Arch. Pharm. Res.* **2003**, *26*, 735–738.
- (26) Nishioka, T.; Watanabe, J.; Kawabata, J.; Niki, R. *Biosci. Biotechnol. Biochem.* **1997**, *61*, 1138–1141.
- (27) Park, J. B. *J. Agric. Food Chem.* **2007**, *6*, 2171–5.
- (28) Stasi, D.; Santos, L. C.; Moreira, E. M. G.; Hiruma, C. C. A. *Revision of Physalis section Epeteiorhiza (Solanaceae), Anales del Instituto de Biología; Universidad Nacional Autónoma de México: São Paulo*, 1989; pp 45–46.
- (29) Martinez, M. *Revision of Physalis section Epeteiorhiza (Solanaceae), Anales del Instituto de Biología; Universidad Nacional Autónoma de México: Serie Botánica*, 1998; Vol. 69, pp 71–117.
- (30) Chang, Y. C.; Chen, C. Y.; Chang, F. R.; Wu, Y. C. *J. Chin. Chem. Soc.* **2001**, *48*, 811–815.
- (31) Jones, G.; Willett, P.; Glen, R. C.; Leach, A. R.; Taylor, R. *J. Mol. Biol.* **1997**, *267*, 727–748.
- (32) Qiu, P.; Yi, M. *Eur. J. Med. Chem.* **2008**, *43*, 604–613.
- (33) Morris, G. M.; Goodsell, D. S.; Halliday, R. S.; Huey, R.; Hart, W. E.; Belew, R. K.; Olson, A. J. *J. Comput. Chem.* **1998**, *14*, 1639–1662.
- (34) Eftink, M. R.; Ghiron, C. A. *Biochemistry* **1976**, *15*, 672–680.
- (35) Sulkowska, A. *J. Mol. Struct.* **2002**, *614*, 227–232.
- (36) Kang, J.; Liu, Y.; Xie, Li, M. S.; Jiang, M.; Wang, Y. *Biochim. Biophys. Acta* **2004**, *1674*, 205–214.
- (37) Kandagal, P. B.; Kalanur, S. S.; Manjunatha, D. H.; Seetharamappa, J. *J. Pharm. Biomed. Anal.* **2008**, *47*, 260–267.
- (38) Lakowicz, J. R. *Principles of Fluorescence Spectroscopy*, 2nd ed.; Kluwer Academic Publishers/Plenum Press: New York, 1999; Vol. 2, pp 237–259.
- (39) Liang, L.; Tajmir-Riahi, H. A.; Subirade, M. *Biomacromolecules* **2008**, *9*, 50–56.
- (40) Zsila, F.; Bikadi, Z.; Simonyi, M. *Biochem. Pharmacol.* **2003**, *65*, 447–456.
- (41) Dufour, C.; Dangles, O. *Biochim. Biophys. Acta* **2005**, *1721*, 164–173.
- (42) Jiang, Y. L. *Bioorg. Med. Chem.* **2008**, *16*, 6406–6414.
- (43) Kanakis, C. D.; Tarantilis, P. A.; Polissiou, M. G.; Diamantoglou, S.; Tajmir-Riahi, A. *J. Mol. Struct.* **2006**, *798*, 69–74.
- (44) Beauchemin, R.; N'soukpo'-Kossi, C. N.; Thomas, T. J.; Thomas, T.; Carpenter, R.; Tajmir-Riahi, H. A. *Biomacromolecules* **2007**, *8*, 3177–3183.
- (45) N'soukpo'e-Kossi, C. N.; Sedaghat-Herati, R.; Ragi, C.; Hotchandani, S.; Tajmir-Riahi, H. A. *Int. J. Biol. Macromol.* **2007**, *40*, 484–490.
- (46) Goormaghtigh, E.; Cabiaux, V.; Ruyschaert, J. M. *Eur. J. Biochem.* **1990**, *193*, 409–420.
- (47) Vandebussche, G.; Clercx, A.; Curstedt, T.; Johansson, J.; Jornvall, H.; Ruyschaert, J. M. *Eur. J. Biochem.* **1992**, *203*, 201–209.

- (48) Ouameur, A. A.; Mangier, E.; Diamantoglou, S.; Rouillon, R.; Carpentier, R.; Tajmir-Riahi, H. A. *Biopolymers* **2004**, *73*, 503–509.
- (49) Kosa, T.; Maruyama, T.; Otagiri, M. *Pharm. Res.* **1998**, *15*, 449–454.
- (50) Abou-Khalil, R.; Jraij, A.; Magdalou, J.; Ouaini, N.; Tome, D.; Greige-Gerges, J. *Photochem. Photobiol., B* **2009**, *95*, 189–195.
- (51) Zunszain, P. A.; Ghuman, J.; McDonagh, A. F.; Curry, S. *J. Mol. Biol.* **2008**, *381*, 394–406.
- (52) Zhang, Y.; Li, Y.; Dong, L.; Li, J.; He, W.; Chen, X.; Hu, Z. *J. Mol. Struct.* **2008**, *875*, 1–8.
- (53) Li, D.; Ji, B.; Sun, H. *Spectrochim. Acta, Part A* **2009**, *73*, 35–40.

JP910156K